

## Supplementary Material for ‘Composite likelihood estimation for the Brown–Resnick process’

BY R. HUSER AND A. C. DAVISON

*Ecole Polytechnique Fédérale de Lausanne, EPFL-FSB-MATHAA-STAT,  
Station 8, 1015 Lausanne, Switzerland*

Raphael.Huser@epfl.ch Anthony.Davison@epfl.ch

### SUMMARY

This document contains details on the computation of the trivariate density for the Brown–Resnick process and supporting simulations and figures for the paper.

#### 1. COMPUTATION OF THE TRIVARIATE DENSITY FOR THE BROWN–RESNICK PROCESS

In three dimensions, the exponent measure may be written as  $V(z_1, z_2, z_3) = I_1/z_1 + I_2/z_2 + I_3/z_3$ , where  $I_k = \Phi_2\{x_k(z_1, z_2, z_3), y_k(z_1, z_2, z_3); R_k\}$  for some differentiable functions  $x_k$  and  $y_k$  of  $z_1, z_2, z_3$  ( $k = 1, 2, 3$ ); see equation (2) of the paper. Therefore, since the trivariate distribution is  $F(z_1, z_2, z_3) = \exp\{-V(z_1, z_2, z_3)\}$ , the density  $f(z_1, z_2, z_3)$  is

$$\begin{aligned} f(z_1, z_2, z_3) &= \frac{d^3}{dz_1 dz_2 dz_3} \exp\{-V(z_1, z_2, z_3)\} \\ &= (-V_{123} + V_1 V_{23} + V_2 V_{13} + V_3 V_{12} - V_1 V_2 V_3) \exp(-V), \end{aligned}$$

where the derivatives  $V_1 = dV(z_1, z_2, z_3)/dz_1$ , etc., are given by expressions such as

$$\begin{aligned} V_1 &= -z_1^{-2} I_1 + z_1^{-1} \frac{dI_1}{dz_1} + z_2^{-1} \frac{dI_2}{dz_1} + z_3^{-1} \frac{dI_3}{dz_1} \\ V_{12} &= -z_1^{-2} \frac{dI_1}{dz_2} + z_1^{-1} \frac{d^2 I_1}{dz_1 dz_2} - z_2^{-2} \frac{dI_2}{dz_1} + z_2^{-1} \frac{d^2 I_2}{dz_1 dz_2} + z_3^{-1} \frac{d^2 I_3}{dz_1 dz_2} \\ V_{123} &= -z_1^{-2} \frac{d^2 I_1}{dz_2 dz_3} + z_1^{-1} \frac{d^3 I_1}{dz_1 dz_2 dz_3} - z_2^{-2} \frac{d^2 I_2}{dz_1 dz_3} + z_2^{-1} \frac{d^3 I_2}{dz_1 dz_2 dz_3} - z_3^{-2} \frac{d^2 I_3}{dz_1 dz_2} + z_3^{-1} \frac{d^3 I_3}{dz_1 dz_2 dz_3}. \end{aligned}$$

By the chain rule, and writing  $x_k = x_k(z_1, z_2, z_3)$ ,  $y_k = y_k(z_1, z_2, z_3)$  for simplicity, we have for  $k, s, t, u = 1, 2, 3$  that

$$\begin{aligned} I_k &= \Phi_2(x_k, y_k; R_k), \\ \frac{d}{dz_s} I_k &= \frac{d}{dx_k} \Phi_2(x_k, y_k; R_k) \frac{dx_k}{dz_s} + \frac{d}{dy_k} \Phi_2(x_k, y_k; R_k) \frac{dy_k}{dz_s}, \\ \frac{d^2}{dz_s dz_t} I_k &= \frac{d^2}{dx_k^2} \Phi_2(x_k, y_k; R_k) \frac{dx_k}{dz_s} \frac{dx_k}{dz_t} + \frac{d^2}{dx_k dy_k} \Phi_2(x_k, y_k; R_k) \left( \frac{dx_k}{dz_s} \frac{dy_k}{dz_t} + \frac{dx_k}{dz_t} \frac{dy_k}{dz_s} \right) \\ &\quad + \frac{d^2}{dy_k^2} \Phi_2(x_k, y_k; R_k) \frac{dy_k}{dz_s} \frac{dy_k}{dz_t} + \frac{d}{dx_k} \Phi_2(x_k, y_k; R_k) \frac{d^2 x_k}{dz_s dz_t} + \frac{d}{dy_k} \Phi_2(x_k, y_k; R_k) \frac{d^2 y_k}{dz_s dz_t}, \end{aligned}$$

$$\begin{aligned}
& \frac{d^3}{dz_s dz_t dz_u} I_k = \frac{d^3}{dx_k^3} \Phi_2(x_k, y_k; R_k) \frac{dx_k}{dz_s} \frac{dx_k}{dz_t} \frac{dx_k}{dz_u} \\
& + \frac{d^3}{dx_k^2 dy_k} \Phi_2(x_k, y_k; R_k) \left( \frac{dx_k}{dz_s} \frac{dx_k}{dz_t} \frac{dy_k}{dz_u} + \frac{dx_k}{dz_s} \frac{dx_k}{dz_u} \frac{dy_k}{dz_t} + \frac{dx_k}{dz_t} \frac{dx_k}{dz_u} \frac{dy_k}{dz_s} \right) \\
& + \frac{d^3}{dx_k dy_k^2} \Phi_2(x_k, y_k; R_k) \left( \frac{dx_k}{dz_s} \frac{dy_k}{dz_t} \frac{dy_k}{dz_u} + \frac{dx_k}{dz_t} \frac{dy_k}{dz_s} \frac{dy_k}{dz_u} + \frac{dx_k}{dz_u} \frac{dy_k}{dz_s} \frac{dy_k}{dz_t} \right) \\
& + \frac{d^3}{dy_k^3} \Phi_2(x_k, y_k; R_k) \frac{dy_k}{dz_s} \frac{dy_k}{dz_t} \frac{dy_k}{dz_u} \\
& + \frac{d^2}{dx_k^2} \Phi_2(x_k, y_k; R_k) \left( \frac{dx_k^2}{dz_s dz_t} \frac{dx_k}{dz_u} + \frac{dx_k^2}{dz_s dz_u} \frac{dx_k}{dz_t} + \frac{dx_k^2}{dz_t dz_u} \frac{dx_k}{dz_s} \right) \\
& + \frac{d^2}{dx_k dy_k} \Phi_2(x_k, y_k; R_k) \left( \frac{dx_k^2}{dz_s dz_t} \frac{dy_k}{dz_u} + \frac{dx_k^2}{dz_s dz_u} \frac{dy_k}{dz_t} + \frac{dx_k^2}{dz_t dz_u} \frac{dy_k}{dz_s} \right. \\
& \quad \left. + \frac{dx_k}{dz_s} \frac{dy_k^2}{dz_t dz_u} + \frac{dx_k}{dz_t} \frac{dy_k^2}{dz_s dz_u} + \frac{dx_k}{dz_u} \frac{dy_k^2}{dz_s dz_t} \right) \\
& + \frac{d^2}{dy_k^2} \Phi_2(x_k, y_k; R_k) \left( \frac{dy_k^2}{dz_s dz_t} \frac{dy_k}{dz_u} + \frac{dy_k^2}{dz_s dz_u} \frac{dy_k}{dz_t} + \frac{dy_k^2}{dz_t dz_u} \frac{dy_k}{dz_s} \right) \\
& + \frac{d}{dx_k} \Phi_2(x_k, y_k; R_k) \frac{d^3 x_k}{dz_s dz_t dz_u} + \frac{d}{dy_k} \Phi_2(x_k, y_k; R_k) \frac{d^3 y_k}{dz_s dz_t dz_u}.
\end{aligned}$$

The derivatives of the bivariate normal cumulative distribution function are easily derived as

$$\begin{aligned}
& \frac{d}{dx} \Phi_2(x, y; \rho) = \phi(x) \Phi \left\{ \frac{y - \rho x}{(1 - \rho^2)^{1/2}} \right\}, \\
& \frac{d^2}{dx^2} \Phi_2(x, y; \rho) = -\phi(x) x \Phi \left\{ \frac{y - \rho x}{(1 - \rho^2)^{1/2}} \right\} - \rho \phi_2(x, y; \rho), \\
& \frac{d^2}{dxdy} \Phi_2(x, y; \rho) = \phi_2(x, y; \rho), \\
& \frac{d^3}{dx^3} \Phi_2(x, y; \rho) = (x - 1) \phi(x) \Phi \left\{ \frac{y - \rho x}{(1 - \rho^2)^{1/2}} \right\} + \rho \phi_2(x, y; \rho) \left( -x^2 + x + \frac{x - \rho y}{1 - \rho^2} \right), \\
& \frac{d^3}{dx^2 dy} \Phi_2(x, y; \rho) = -\phi_2(x, y; \rho) \frac{x - \rho y}{1 - \rho^2},
\end{aligned}$$

with the others defined by symmetry, and the non-zero derivatives of  $x_k(z_1, z_2, z_3)$  and  $y_k(z_1, z_2, z_3)$  with respect to  $z_1, z_2, z_3$  are given for  $n = 1, 2, \dots$  by

$$\begin{aligned}
& \frac{d^n x_1}{dz_1^n} = (n - 1)! (-z_1)^{-n} \gamma_{12}^{-1/2}, & \frac{d^n x_1}{dz_2^n} = -(n - 1)! (-z_2)^{-n} \gamma_{12}^{-1/2}, \\
& \frac{d^n y_1}{dz_1^n} = (n - 1)! (-z_1)^{-n} \gamma_{13}^{-1/2}, & \frac{d^n y_1}{dz_3^n} = -(n - 1)! (-z_3)^{-n} \gamma_{13}^{-1/2}, \\
& \frac{d^n x_2}{dz_1^n} = -(n - 1)! (-z_1)^{-n} \gamma_{12}^{-1/2}, & \frac{d^n x_2}{dz_2^n} = (n - 1)! (-z_2)^{-n} \gamma_{12}^{-1/2},
\end{aligned}$$

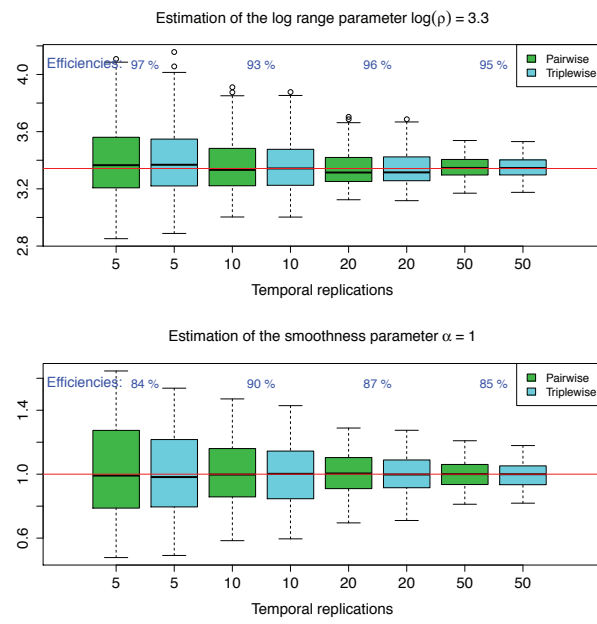


Fig. 1. Boxplots of the 300 independent estimates of the log-range parameter (top) and smooth parameter (bottom), as the number of temporal replicates  $n$  increases. Green and blue boxes correspond respectively to  $\hat{\theta}_2$  and  $\hat{\theta}_3$ . The horizontal red lines correspond to the true values  $\log(\rho) \approx 3.3$ , i.e.,  $\rho = 28$ , and  $\alpha = 1$ . The relative efficiencies  $\hat{RE}_\rho$  and  $\hat{RE}_\alpha$  are also reported.

$$\begin{aligned} \frac{d^n y_2}{dz_2^n} &= (n-1)!(-z_2)^{-n}\gamma_{23}^{-1/2}, & \frac{d^n y_2}{dz_3^n} &= -(n-1)!(-z_3)^{-n}\gamma_{23}^{-1/2}, \\ \frac{d^n x_3}{dz_1^n} &= -(n-1)!(-z_1)^{-n}\gamma_{13}^{-1/2}, & \frac{d^n x_3}{dz_3^n} &= (n-1)!(-z_3)^{-n}\gamma_{13}^{-1/2} \\ \frac{d^n y_3}{dz_2^n} &= -(n-1)!(-z_2)^{-n}\gamma_{23}^{-1/2}, & \frac{d^n y_3}{dz_3^n} &= (n-1)!(-z_3)^{-n}\gamma_{23}^{-1/2}, \end{aligned}$$

## 2. SUPPORTING FIGURES

Figure 1 below suggests that in a typical situation, with  $\rho = 28$  and  $\alpha = 1$ ,  $\hat{\theta}_2$  and  $\hat{\theta}_3$  estimate  $\theta$  consistently as  $n \rightarrow \infty$ , and that their relative efficiency is quite stable with  $n$ . As Table 1 of the paper indicates, this is also true for other values of  $\rho$  and  $\alpha$ , except for  $\alpha = 2$ . Figure 2 below illustrates the super-efficiency of  $\hat{\theta}_3$  when  $\alpha = 2$ . Figure 3 suggests that the correlation matrices  $R_k$  in expression (2) of the paper may be numerically singular when  $\alpha \approx 2$ , especially for large  $p$ . In fact, they are exactly singular when  $\alpha = 2$  and  $p > d + 1$ .

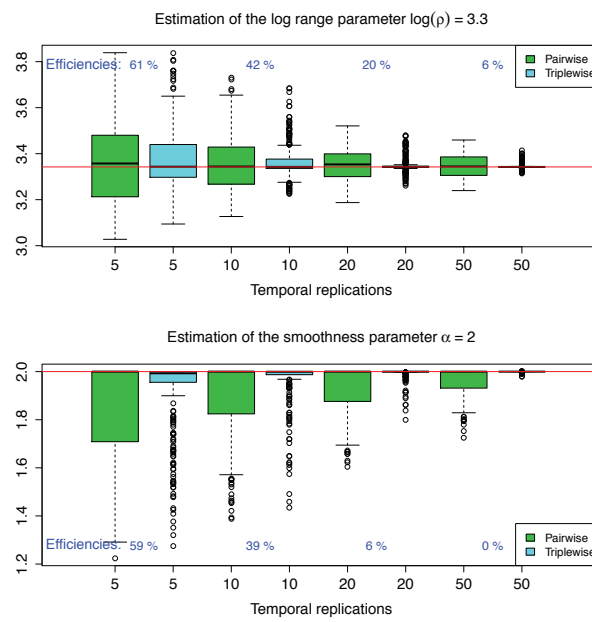


Fig. 2. Boxplots of the 300 independent estimates of the log-range parameter (top) and smooth parameter (bottom), as the number of temporal replicates  $n$  increases. Green and blue boxes correspond respectively to  $\hat{\theta}_2$  and  $\hat{\theta}_3$ . The horizontal red lines correspond to the true values  $\log(\rho) \approx 3.3$ , i.e.,  $\rho = 28$ , and  $\alpha = 2$ . The relative efficiencies  $\text{RE}_\rho$  and  $\text{RE}_\alpha$  are also reported.

### 3. EFFICIENCIES WITH INCREASING NUMBER OF LOCATIONS

Table 1 below suggests that when  $\alpha < 2$ , the efficiency of triplewise likelihood estimators is rather stable with the number of locations  $S$ , but when  $\alpha = 2$ , corresponding to the Smith model, the efficiency decreases rapidly with  $S$ ; presumably this is also the case when  $\alpha \approx 2$ .

### ACKNOWLEDGEMENT

This research was funded by the Swiss National Science Foundation, and partly performed in the context of the ETH Competence Center Environment and Sustainability (CCES).

[Received January 2011. Revised June 2011]

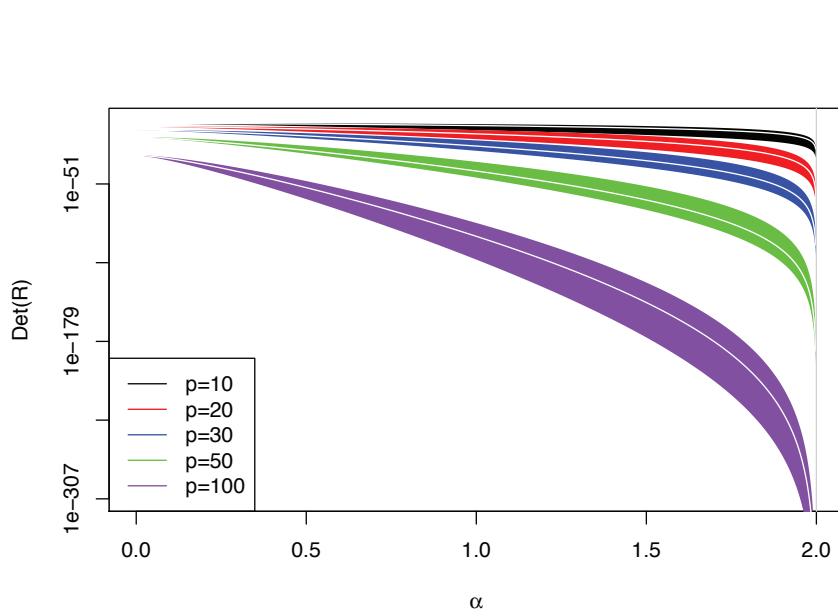


Fig. 3. Determinant of the correlation matrix  $R_1$  in expression (2) of the paper against the smoothness parameter  $\alpha \in (0, 2]$  when the range parameter  $\rho$  equals 100, for  $d = 2$  and  $p = 10$  (black), 20 (red), 30 (blue), 50 (green) and 100 (purple). The colored areas correspond to 95% confidence regions, while the white lines denote the medians based on 50 simulated locations in  $[0, 100]^2$ .

Table 1. Efficiency (%) of maximum pairwise likelihood estimators relative to maximum triplewise likelihood estimators for  $n = 20$ , based on 300 simulations of the Brown-Resnick process with semi-variogram  $(\|h\|/\rho)^\alpha$  observed at  $S = 10, 20, 30, 50$  random sites in  $[0, 100]^2$ . The numbers are respectively  $RE_\rho/RE_\alpha/RE_\theta$ .

$\alpha \setminus \rho$	$S = 10$			$S = 20$		
	14	28	42	14	28	42
0.5	97/96/96	93/92/92	94/97/95	95/94/93	93/96/95	93/96/94
1.0	94/85/90	95/84/89	96/86/91	94/85/90	95/89/93	95/90/93
1.5	88/83/88	92/64/74	91/64/74	92/78/85	91/68/76	89/69/77
2.0	75/75/75	42/37/36	26/14/15	55/62/56	24/19/21	11/0/2
S = 30						
$\alpha \setminus \rho$	14			28		
	91/93/92	90/92/92	89/95/92	89/93/91	88/93/91	89/94/92
0.5	98/86/92	95/84/90	92/87/92	96/84/90	94/87/93	93/90/93
1.0	94/81/86	92/70/78	89/72/79	96/77/84	90/69/81	88/67/79
1.5	54/50/50	24/9/12	9/0/2	47/39/41	15/4/7	5/0/1